CONFIGURATION SPACES
AND LIMITS OF VORONOI DIAGRAMS

RODERIK LINDENBERGH

Department of Mathematical Geodesy and Positioning, Delft University of Technology
P.O.Box 5058, 2600 GB Delft, The Netherlands
E-mail: r.c.lindenbergh@geo.tudelft.nl

WILBERD van der KALLEN and DIRK SIERSMA

Department of Mathematics, Utrecht University
P.O.Box 80010, 3508 TA Utrecht, The Netherlands
E-mail: W.vanderKallen@math.uu.nl, D.Siersma@math.uu.nl

Abstract. The Voronoi diagram of n distinct generating points divides the plane into cells, each of which consists of points most close to one particular generator. After introducing 'limit Voronoi diagrams' by analyzing diagrams of moving and coinciding points, we define compactifications of the configuration space of n distinct, labeled points. On elements of these compactifications we define Voronoi diagrams.

1. Introduction. The Voronoi diagram of a set S of n distinct points in $\mathbb{R}^2$ associates to a point $p \in S$ that part of the plane that is closer to p than to any other point in S. Voronoi diagrams are one of the major structures investigated in Computational geometry, see [1, 2]. Applications can be found in e.g. astronomy, cartography, computer vision, theoretical physics, etc., see also [8]. We treat Voronoi diagrams however from a more mathematical viewpoint: in this overview article we consider moving points and demonstrate ways to define Voronoi diagrams for point sets that may contain coinciding points. We present methods, example and theorems here; for full proofs and background information, please consult the dissertation of the first author [7]. All results in this paper and in [7] generalize in appropriate sense to higher dimensions and to weighted distance functions.

2. Voronoi diagrams

2.1. *Definitions.* Let $S = \{p_1, \ldots, p_n\}$ with $p_i \in \mathbb{R}^2$ and $p_i \neq p_j$ if $i \neq j$. The *Voronoi cell* of p_i is given by

$$V(p_i) = \{q \in \mathbb{R}^2 : \|p_i - q\| \leq \|p_j - q\|, \ i \neq j\}.$$

The *Voronoi diagram* is the family of subsets of $\mathbb{R}^2$ consisting of the Voronoi cells and all of their intersections.

The *Voronoi half-plane* $vh(p_i, p_j)$ is given by

$$vh(p_i, p_j) = \{q \in \mathbb{R}^2 : \|p_i - q\| \leq \|p_j - q\|\}.$$

It is bounded by the *bisector* $B(p_i, p_j)$ of p_i and p_j. The next lemma shows that the Voronoi cell of p_i is characterized by the Voronoi half-planes $vh(p_i, p_j)$.

LEMMA 1. $V(p_i) = \bigcap_{j \neq i} vh(p_i, p_j)$.

2.2. *Small diagrams.* In Figure 1, all possible Voronoi diagrams with 2, 3, or 4 points are shown. Here, we only distinguish Voronoi diagrams that are combinatorially distinct, and, moreover, we ignore the labelling of the vertices.
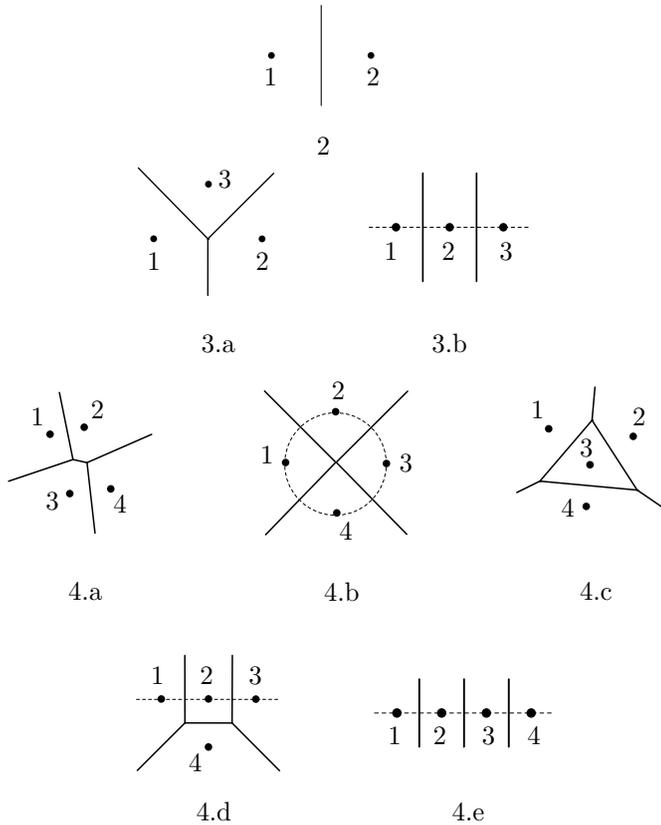
Figure 1. Voronoi diagrams on two, three and four points.

In these cases we can distinguish between generic situations, e.g. where the Voronoi diagrams do not change if we move the sites slightly, and the non-generic diagrams, where this is not the case. Diagrams 2, 3.a, 4.a, and 4.c are generic, the others are non-generic.

2.3. *Perestroika's between generic situations.* Assume the points defining the Voronoi diagrams are allowed to move. We are interested in perestroika's between two generic situations. We distinguish two special events that we describe using Voronoi circles. In these events only four points of S are involved, denoted by a, b, c, and d. The circle passing through a, b and c is denoted by C_{abc}. A circle passing through three points of the generating set S is an *empty circle* if it contains no points of S in its interior.

The first event is when two empty circles C_{abd} and C_{bcd} coincide. This is a *circle event*, see Figure 2. Before the event, a, b, c, and d define two empty circles C_{abd} and C_{bcd}. If c moves to the left in the leftmost figure, a, b, c and d become cocircular. If c continues moving left, one arrives at the situation of the rightmost figure, where C_{abc} and C_{acd} are the empty circles.
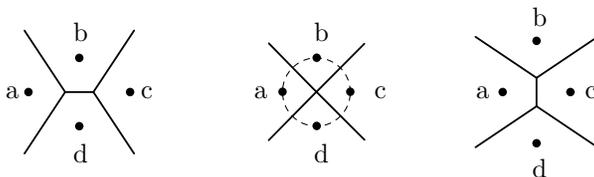
Figure 2. A circle event.

The other way by which a generic Voronoi diagram can change is by means of a convex hull event, see Figure 3. Consider the circle defined by the points a, b and c. In the figure on the left, b is on the convex hull of S. The circle C_{abc} contains all other points of S in its interior. Suppose b moves to the left. At some stage, b passes through the line segment ab. At this moment, the circle C_{abc} swaps over, and becomes empty, as in the picture on the right.
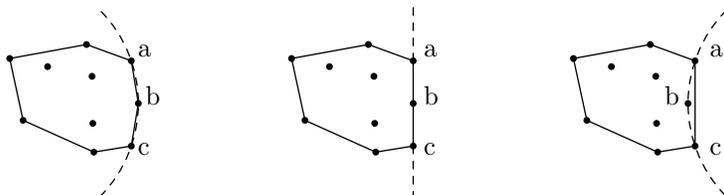
Figure 3. A convex hull event.

The circle event and the convex hull event are the only perestroika's (bifurcations) of Voronoi diagrams, which occur in generic one-parameter families of moving points. More complicated bifurcations are e.g. related to five points on a circle or four points on one edge of the convex hull (these and others occur as bifurcations in generic two parameter families).

3. Polynomial sites and their Voronoi diagram

3.1. *Points moving at distinct speeds and directions.* We model points moving at distinct speed by differentiable curves $p_i(t)$, defined for a finite common interval of the real line, say $[-r, +r]$. That is, we consider

$$S(t) = \{p_1(t), \ldots, p_n(t)\}.$$

We include the possibility that for $t = 0$ one or more points coincide, but still assume that they are different if $t \neq 0$. We also assume that the differences $p_i(t) - p_j(t)$ have a non-vanishing (higher) derivative at $t = 0$. For convenience we assume that all $p_i(t)$ are polynomial. We call such $p_i(t)$ *polynomial sites.*

We use the characterization of Voronoi cells by means of half-planes for defining Voronoi diagrams for polynomial sites. Let $u(t)$ and $v(t)$ be two polynomial sites. We can define a Voronoi half-plane for $u(t)$ and $v(t)$ when we know both the (oriented) direction and one point of the bisector bounding the half-plane.

This one point is given by the *bisection point* $b_0(u, v) = (b_x, b_y)$ of $u(t)$ and $v(t)$ at $t = 0$ and is defined by

$$b_0(u, v) = \tfrac{1}{2}\big(u(0) + v(0)\big).$$

The *direction* ϕ_{uv} at $t = 0$ is the angle in $\mathbb{R}/2\pi\mathbb{Z}$ of the line segment $v(t) - u(t)$ at $t = 0$. In this definition of ϕ_{uv} we take the limit for small positive t of the direction of the directed line that passes first through $u(t)$ and then through $v(t)$. We could of course also have chosen the limit from the other side. Let **n** be any non-zero vector, pointing in the direction ϕ_{uv}. The Voronoi half-plane $vh(u, v)$ is the half-plane defined by

$$\mathbf{n} \cdot (x - b_x, y - b_y) \leq 0.$$

We next take $V(p_i) = \bigcap_{j \neq i} vh(p_i, p_j)$ as definition of the Voronoi diagram of a set of polynomial sites at $t = 0$ and call them *limit diagrams.*

3.2. *Properties and small examples of limit diagrams.* Limit diagrams share many properties with ordinary Voronoi diagrams, for example the convexity of the cells, but there are some interesting differences:

- Limit Voronoi cells can have area zero.
- Limit Voronoi cells can have diameter zero.
- Limit diagrams for $t > 0$ and for $t < 0$ can be different.
- Limit diagrams can have a "hidden" combinatorial structure.

This new behaviour is demonstrated in Figures 4 and 5, where we list all limit diagrams with 2 or 3 coinciding points.

Figure 4. Limit Voronoi diagram for negative and positive t.

For two points there is essentially one new diagram that we get by generalizing to limit diagrams. It occurs whenever two polynomial sites coincide, and is fully determined by the direction ϕ_{uv} of the two polynomial sites u and v involved.

Suppose that $p_1(t) = (0,0)$ and $p_2(t) = (t,0)$. Then t can approach zero from both the negative and the positive side. The resulting diagrams are given in Figure 4.
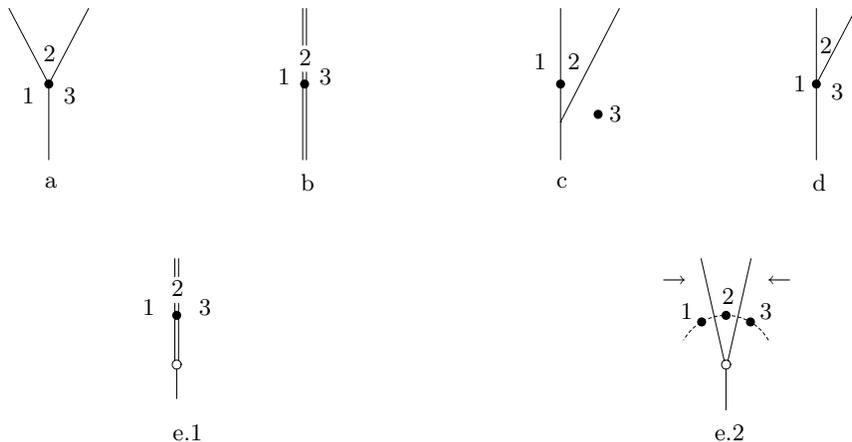
Figure 5. Five limit Voronoi diagrams for three points.

A generic limit diagram of three coinciding points is given in Figure 5.a. In Figure 5.b one can think of three collinear sites that shrink to one point. Note that the cell of site 2 has zero area. Figures 5.b and 5.e.1 show what is meant by 'hidden' combinatorics. Both pictures just look like one straight line, although Figure 5.b consists in fact of two coinciding lines, while 5.e.1 comes from a vertex with three arcs (see Figure 5.e.2) where two arcs coincide.

3.3. *A diameter zero cell and more hidden combinatorics.* On the left in Figure 6, a Voronoi diagram of type 4.c (compare Figure 1) is shown. If one scales this diagram to zero distances then the limit diagram of the four sites is shown on the right in Figure 6. A parametrization of the sites is given by $q_1(t) = (2t, 2t^3)$, $q_2(t) = (-2t, 2t)$, $q_3(t) = (-2t^2, -3t)$, and $q_4(t) = (t^2, -t^4)$.

Figure 6. The Voronoi diagram of the points $q_1(t), q_2(t), q_3(t)$ and $q_4(t)$ for small positive t and at $t = 0$.

Another example of nice hidden combinatorics is given in Figure 7. It displays schemat-
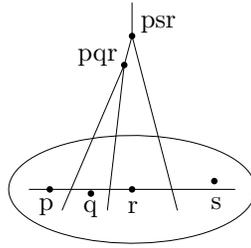
Figure 7. Edge of zero length outside $(0,0)$.

ically a limit diagram that looks just like a line. In this limit diagram the Voronoi edge $e(p,r)$ gets zero length, while it is situated at the point $(0,2)$, although all sites coincide in $(0,0)$. A parametrization of the sites involved is given by $p(t) = (-2t, 0)$, $q(t) = (-t, -\frac{1}{4}t^2)$, $r(t) = (0,0)$, and $s(t) = (2t, 2t^2)$.

3.4. *Plugging.* If all sites in $S(0)$ are different, then the limit Voronoi diagram coincides with the (ordinary) Voronoi diagram of $S(0)$. If at $t = 0$ there is a collision at distinct locations $S(0) = \{l_1, \ldots, l_m\}$ where the l_j are pairwise distinct, then one can compute the limit diagram in three steps:

1. Compute the (ordinary) Voronoi diagram of $l_1, \ldots, l_m$.

2. Compute for each j $(j = 1, \ldots, m)$ the limit Voronoi diagram of the set of sites $p_i(t)$ with limit l_k.

3. 'Plug in' the limit diagrams, obtained in Step 2, at the corresponding Voronoi cell of l_k. The plugging is illustrated in Figure 8.
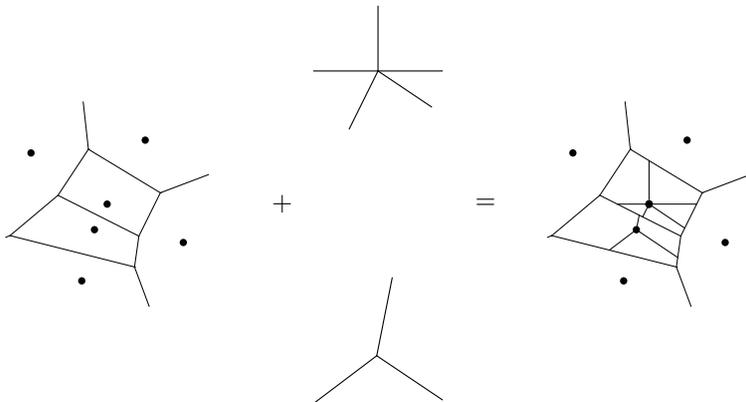
Figure 8. Plugging diagrams.

At the end of this paragraph we conclude that we have found a new class of mathematical objects, limit Voronoi diagrams, that contains all ordinary Voronoi diagrams but, moreover, contains certain limit diagrams that cannot be realized as ordinary Voronoi
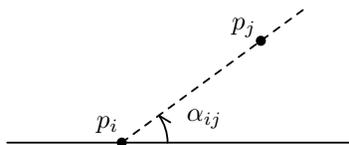
Figure 9. The angle α_{ij} of two points p_i and p_j.

diagrams. We have also seen that we need angles modulo 2π in order to define Voronoi diagrams out of Voronoi half-planes. And certain cells disappear in the limit. In order to make these cells visible, we need some relation between scale and shape.

4. Compactifying the configuration space

4.1. *Angles and points compactification.* The *configuration space* of n distinct labelled points in $\mathbb{R}^2$ is the set $CONF_n \subset (\mathbb{R}^2)^n$ given by

$$CONF_n = \{(p_1, \ldots, p_n) : p_i \neq p_j \text{ if } i \neq j\}.$$

So, a configuration is just a set of distinct points in the plane. For any two distinct points p_i and p_j, the *directed angle* $\alpha_{ij} \in \mathbb{R}/2\pi\mathbb{Z}$ is the argument of the point

$$(\cos \alpha_{ij}, \sin \alpha_{ij}) = \Big(\frac{d_x}{\|d_x\|}, \frac{d_y}{\|d_y\|}\Big),$$

where $d = (d_x, d_y) := p_j - p_i$, see Figure 9. The *undirected angle* $\overline{\alpha_{ij}}$ is defined as $\overline{\alpha_{ij}} = \overline{\alpha_{ji}} = \alpha_{ij} \bmod \pi$. For a configuration c in $CONF_n$ we can determine the set a_n of angles mod 2π of lines through any two points in c. That is, we define a map ψ_{DA_n}, given by

$$\begin{aligned} \psi_{\mathrm{DA}_n} : \quad CONF_n &\to (\mathbb{R}/2\pi\mathbb{Z})^{\binom{n}{2}}, \\ (p_1, \ldots, p_n) &\mapsto \big(\alpha_{ij}\big)_{1 \leq i < j \leq n}. \end{aligned}$$

The *angles and points compactification* CDA_n is the closure of the graph of ψ_{DA_n} in $(\mathbb{R}^2)^n \times (\mathbb{R}/2\pi\mathbb{Z})^{\binom{n}{2}}$.

In an analogous way we define the map ψ_{UA_n} from $CONF_n$ to the undirected angles and the corresponding undirected compactification CUA_n.

An example of an element or data set of CDA_2 is given by $\big((0,0),(0,0),\frac{\pi}{6}\big)$. It is a degenerate configuration of two coinciding points p_1 and p_2 such that $\alpha_{12} = \frac{\pi}{6}$. Another example is $\big((0,0),(\frac{1}{2}\sqrt{3}, \frac{1}{2}), \frac{\pi}{6}\big)$. In this case $p_1 = (0,0)$ and $p_2 = \big(\frac{1}{2}\sqrt{3}, \frac{1}{2}\big)$. From this it follows already that $\alpha_{12} = \frac{\pi}{6}$, as this is a non-degenerate configuration.

4.2. *An algebraic counterpart of the compactification.* In the next section we are going to show that the definition of Voronoi diagram extends to CDA_n. We first want to answer the question:

Are CUA_n and CDA_n smooth manifolds?

Moreover, we are interested in their algebraic counterparts. In this section we describe an algebraic variety T_n that is very similar to CUA_n. We know that $CONF_n$ is contained in CUA_n: by definition, CUA_n equals the closure of the graph of the undirected angle

map:

$$CONF_n \subset CUA_n \subset \left(\mathbb{R}^2\right)^n \times (\mathbb{R}/\pi\mathbb{Z})^{\binom{n}{2}}.$$

Therefore, CUA_n contains a '$CONF_n$ part' that is smooth. The remaining points of CUA_n lie above the *diagonal* $\Delta \subset (\mathbb{R}^2)^n$ consisting of configurations with at least two coinciding points p_i and p_j. We make an algebraic description for $\mathbb{R}/\pi\mathbb{Z} = \mathbb{P}^1$ by taking coordinates $(a_{ij} : 1)$ and $(1 : b_{ij})$, where

$$a_{ij} = \tan\overline{\alpha}_{ij}; \qquad b_{ij} = \frac{1}{\tan\overline{\alpha}_{ij}}.$$

For simplicity, we consider only the case where $b_{ij} \neq 0$ on each $\mathbb{P}^1$, so we work on the $(a_{ij} : 1)$-chart. We have transformed ψ_{UA_n} in a rational map ψ_{slope} given by

$$\psi_{\mathrm{slope}}\big((x_0, y_0), \ldots, (x_{n-1}, y_{n-1})\big) = \left\{\left(\frac{y_j - y_i}{x_j - x_i}\right)\right\}_{0 \leq i < j \leq n-1},$$

where $\big((x_0, y_0), \ldots, (x_{n-1}, y_{n-1})\big) \in CONF_n$. Without loss of generality we assume in this section that $x_0 = y_0 = 0$. That is, we consider configurations up to translation. The dimension of $CONF_n(\mathbb{R}^2)$ up to translations equals $2n - 2$. The slope a_{0i}, for $i \in \{1, \ldots, n-1\}$, is denoted shortly by a_i. The triangle T_{ij} is the triangle with vertices (x_0, y_0), (x_i, y_i), and (x_j, y_j). The following lemma shows that there exists a relation between the x-coordinates of the vertices of T_{ij} and the slopes of the lines bounding T_{ij}. Let

$$t_{ij} = a_i x_i - a_j x_j - a_{ij} x_i + a_{ij} x_j.$$

Observe that $t_{ij} = 0$ on the $(a_{ij} : 1)$-chart of $CONF_n$. Moreover, on this chart we have $CUA_n \subset \{t_{ij} = 0\}$ for $1 \leq i < j \leq n - 1$. A question is if equality holds. That is, if the closed algebraic set $\{t_{ij} = 0\}_{1 \leq i < j \leq n-1}$ is contained in CUA_n. The answer is no. We prove this later on by means of the six-slopes formula:
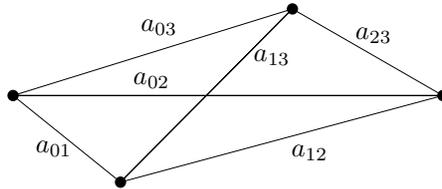
Figure 10. For four distinct points the six-slopes formula holds.

LEMMA 2 (six-slopes formula). *Let p_0, p_1, p_2 and p_3 be distinct points in the plane. Then $\Delta = \Delta_{0123} = 0$, where Δ is given by*

$$\Delta = (a_1 - a_{12})(a_2 - a_{23})(a_3 - a_{13}) - (a_1 - a_{13})(a_2 - a_{12})(a_3 - a_{23}).$$

Proof. In the generic situation it is clear that one of the slopes can be computed in terms of the others. Do so. The formula is also true in the limit. ∎

Note that interchanging indices $1 \leftrightarrow 2$, etc., changes the appearance of the expression for Δ_{0123}, but does not change the expression itself. By Δ_{ijkl} we denote Δ_{0123} with 0, 1, 2 and 3 replaced by i, j, k and l.

COROLLARY 3. $\Delta_{ijkl} = 0$ *on* CUA_n.

Instead of just looking at the zeros of $t_{ij} = 0$, we add the condition that all Δ_{ijkl} equal zero as well. This leads to the following definition.

The *triangle variety* T_n is the set of common zeroes of the polynomials t_{ij} for $1 \le i < j \le (n-1)$ and Δ_{ijkl} for $0 \le i < j < k < l \le (n-1)$. Any variable, of the form a_{ij} or x_i, takes value in $\mathbb{R}$.

The zero set of the polynomials $f_1 \ldots, f_n$ is indicated by $V(f_1, \ldots, f_n)$. So $T_4 = V(t_{12}, t_{13}, t_{23}, \Delta_{123})$.

4.3. *Singularities of the triangle variety for small* n. In this section we determine singularities of the triangle variety T_n for $n = 3$ and $n = 4$. We start with $n = 3$.
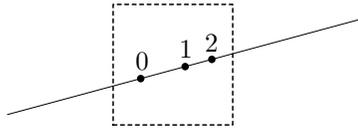
Figure 11. Three coinciding points with coinciding directions.

LEMMA 4. *An element* $c = (x_0, x_1, x_2, a_1, a_2, a_{12}) \in T_3$ *is singular iff all points and all slopes coincide. That is*:

$$x_0 = x_1 = x_2, \qquad and \qquad a_1 = a_2 = a_{12}.$$

The type of this singularity is A_∞.

Proof. Note that $t_{12} = (a_1 - a_{12})x_1 + (a_{12} - a_2)x_2 = 0$. From this it follows that the singular set is given by $a_i = a_j = a_{ij}$, and that the singularity is of type A_∞, cf. [9] (smooth one-dimensional singular locus with transversal type Morse (A_1)). ■

Geometrically, the singularities of T_3 correspond to degenerated configurations where all three points coincide and the directions between the three points coincide, see Figure 11.

Next we consider $n = 4$.

PROPOSITION 5. $CUA_4 \ne V(t_{12}, t_{13}, t_{23})$.

Proof. The variety $V(t_{12}, t_{13}, t_{23})$ contains $0 = x_1 = x_2 = x_3$ as a component, *without* the condition that $\Delta_{0123} = 0$. ■

This explains why we have added the Δ_{ijkl}'s in the definition of the triangle variety T_n.

LEMMA 6. *A configuration* $c \in T_4$ *is singular iff, up to relabelling, both* $x_0 = x_1 = x_2$ *and* $a_1 = a_2 = a_{12}$.

Figure 12. Typical singular configuration: three coinciding, collinear points with a fourth point.

The singularities of T_4 are closely related to the singularities of T_3. If only three points coincide, including their slopes, we have a singularity of type A_∞, just as for T_3. But if all points coincide a more complicated singularity occurs as several A_∞ singularities 'meet': one can move any of the four points away in such a way that the three remaining points are as in the configuration of Lemma 4.

It is still an open question whether $CUA_4 = T_4$. Maybe we need to add some relations or inequalities to T_4 to obtain equality?

5. A stability theorem. For data sets γ_n in the angles and hook compactification CDA_n, limit Voronoi diagrams are defined, just as for polynomial sites: for every two points $p_i = p_j$ the Voronoi half-plane $vh(p_i, p_j)$ is the half-space through $p_i = p_j$ determined by α_{ij}. Using our characterization of Voronoi cells by half-planes, we write $V(p_i) = \bigcap_{j \neq i} vh(p_i, p_j)$ for the Voronoi cell of p_i. This gives us a Voronoi diagram $V(\gamma_n)$ for every $\gamma_n \in CDA_n$.

If we want to compare two Voronoi diagrams, a suitable notion of distance is the Hausdorff distance: two sets A and B are within *Hausdorff distance* r iff r is the smallest number such that any point of A is within distance r from some point of B and vice versa. If we compare two Voronoi diagrams in the Hausdorff distance, we mean that we compare the common boundary of the Voronoi cells or the one-skeleton of the diagrams.

We know by now that we can represent a Voronoi diagram of a set of non-necessarily distinct points in the plane by data sets consisting of the coordinates of the points and the pairwise angles α_{ij} between the points. It even turns out that this representation by coordinates and angles is stable with respect to the Hausdorff metric if we put a mild restriction on the point configurations allowed.

More precisely, we only allow point configurations on the *unit disk* $\mathcal{U} := \{x \in \mathbb{R}^2 : \|x\| \leq 1\}$. These point configurations are monitored by four additional so-called *camera points* $c_1 = (-N, 0)$, $c_2 = (0, N)$, $c_3 = (N, 0)$ and $c_4 = (0, -N)$. If $N \gg 1$ is chosen big enough and if only the points within the unit disk are allowed to move, then we get enough control to prove the following theorem on the restricted configuration space

$$CDA_n^{\mathcal{U}} := \{c_1, \ldots, c_4; \, p_1, \ldots, p_n; \, \alpha_{12}, \ldots, \alpha_{(n+3)(n+4)}\},$$

with $p_i \in \mathcal{U}$ and $\alpha_{ij} \in \mathbb{R}/2\pi\mathbb{Z}$.

THEOREM 7. *Let* $\gamma_n \in CDA_n^{\mathcal{U}}$. *Then the Voronoi diagram* $V(\eta_n)$ *of any data set* $\eta_n \in CDA_n^{\mathcal{U}}$ *that is Euclidean-close to* γ_n, *is Hausdorff-close to the Voronoi diagram* $V(\gamma_n)$:

$$\forall \epsilon > 0 \; \exists \delta > 0 \; \big[d(\gamma_n, \eta_n) \leq \delta \Rightarrow h(V(\gamma_n), V(\eta_n)) \leq \epsilon \big]$$

Proof. See [7]. ∎

6. Clickable diagrams in a clickable compactification. In this paragraph we describe shortly a different compactification that has two big advantages compared to the angles and points compactification CDA_n. First, it is smooth as a manifold, and second, it has a natural recursive structure. We exploit this structure to introduce clickable Voronoi diagrams for clickable configurations.
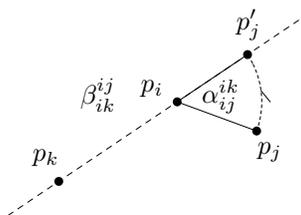
Figure 13. Constructing p_k out of p_i and p_j.

6.1. *A smooth angles and hooks compactification.* Such a clickable configuration is described by a set of data encoding the locations of the points and, if two or more points coincide a *screen* is specified for the set of labels of coinciding points. This compactification is a real version of the famous Fulton-MacPherson compactification [4], that is described in terms of distinct points in a nonsingular algebraic variety.

We consider point configurations up to scalings, s, and translations, t. That is, our point configurations live in the *reduced* configuration space

$$conf_n = CONF_n / \{s, t\}.$$

Kontsevich and Soibelman, [5, 6], define the manifold with corners $FM_2(n)$ as the closure of the image of $conf_n$ in the compact manifold $(S^1)^{\binom{n}{2}} \times [0, \infty]^{6\binom{n}{3}}$ under the map

$$\big[(p_1, \ldots, p_n)\big] \mapsto \big((\alpha_{ij})_{1 \leq i < j \leq n}, \beta_{ij}^{ik}\big),$$

where i, j and k pairwise distinct. β_{ij}^{ik} denotes the *ratio* $\frac{|p_i - p_k|}{|p_i - p_j|}$.

Instead of just a ratio, we specify for every triple of points a *hook* $h_{ij}^{ik} = (\beta_{ij}^{ik}, \alpha_{ij}^{ik})$ that tells how to construct the point p_k, given the points p_i and p_j, see Figure 13. Here, both the hooks $(\beta_{ij}^{ik}, \alpha_{ij}^{ik})$ and $(-\beta_{ij}^{ik}, \alpha_{ij}^{ik} + \pi)$ 'construct' the same point p_k. This gives us an equivalence relation

$$\big(\beta_{ij}^{ik}, \alpha_{ij}^{ik}\big) \sim_K \big(-\beta_{ij}^{ik}, \alpha_{ij}^{ik} + \pi\big).$$

Note that we emphatically allow negative "ratio's". Let

$$AH_n = (\mathbb{R}/\pi\mathbb{Z})^{\binom{n}{2}} \times \big(([-\infty, \infty] \times \mathbb{R}/2\pi\mathbb{Z})/ \sim_K\big)^{6\binom{n}{3}}$$

and define the *angles and hooks compactification* XAH_n as the closure of the image of the map

$$\psi_{AH_n} : \quad \begin{array}{c} conf_n \\ [(p_1, \ldots, p_n)] \end{array} \quad \begin{array}{c} \to AH_n, \\ \mapsto \big((\overline{\alpha_{ij}})_{i<j}, (h_{ij}^{ik})\big) \end{array}$$

where i, j and k pairwise distinct.

THEOREM 8. *XAH_n is a smooth submanifold of AH_n.*

Proof. See [7]. ∎

6.2. *Filling screens.* Now suppose we are given some x in XAH_n or in $FM_2(n)$. We can determine a family of screens—the x-screens—by analyzing zero ratios, that is, ratios of the form $\frac{p_i - p_k}{p_i - p_j} = 0$: this particular zero ratio for example, tells that p_i and p_k can be thought of as coinciding points from p_j's viewpoint. Next pick a set of hooks and angles
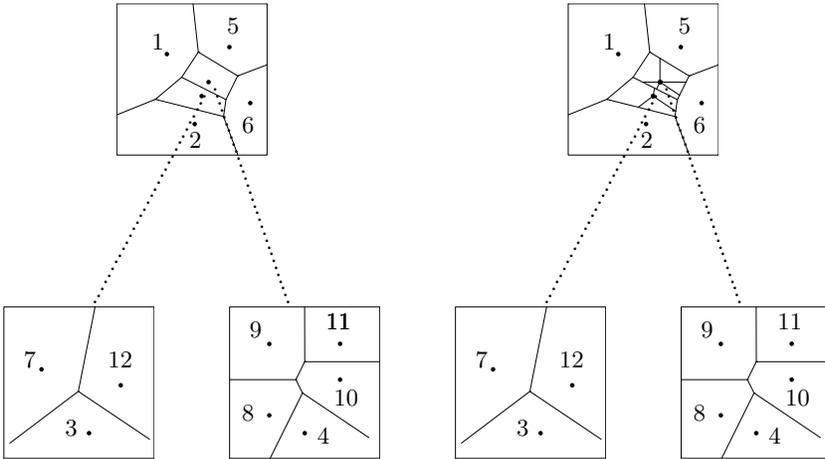
Figure 14. Clickable Voronoi diagrams in clickable configurations.

that is sufficient to fix all relative positions in all screens. Finally fill the screens using this set of hooks and angles. As a result, any two points are separated in some screen.

6.3. *Adding Voronoi diagrams.* We add clickable Voronoi diagrams in the filled x-screens for $x \in FM_2(n)$ in two steps that are illustrated in Figure 14.

1. In any filled x-screen all points are separated. So we can add the ordinary Voronoi diagrams of the points displayed, see Figure 14, on the left.

2. Add the Voronoi diagram of some x-screen S to the cell corresponding to S in the x-screen T just above S. This recursive step should start at the lowest screens, compare Figure 14, on the right.

6.4. *Polynomial sites versus $FM_2(n)$.* We have already shown how to define pairwise angles for a set of polynomial sites. In a similar way, we can define ratios for triples of polynomial sites. This shows how to map a set of polynomial sites to a data set in $FM_2(n)$.

On the other hand, from $x \in FM_2(n)$ we can construct a set of n polynomial sites by reading off coordinates of points in appropriate screens, by using a natural predecessor relation on the labels $1, \ldots, n$ and by adding t's if the depth of the x-screens increases.

Combining these two steps defines a normal form for the polynomial sites.

References

[1] F. Aurenhammer, R. Klein, *Voronoi diagrams*, in: Handbook of Computational Geometry, J.-R. Sack, J. Urrutia (eds.), North-Holland, Amsterdam, 2000, 201–290.

[2] M. de Berg, M. van Kreveld, M. Overmars, O. Schwarzkopf, *Computational Geometry*, Springer, Berlin, 1997.

[3] H. Edelsbrunner, *Geometry and Topology of Mesh Generation*, Cambridge Univ. Press, Cambridge, 2001.

[4] W. Fulton, R. MacPherson, *A compactification of configuration spaces*, Ann. of Math. (2) 139 (1994), 183–225.

[5] M. Kontsevich, *Operads and motives in deformation quantization*, Lett. Math. Phys. 48 (1999), 35–72.

[6] M. Kontsevich, Y. Soibelman, *Deformation of algebras over operads and the Deligne conjecture*, in: Conférence Moshé Flato 1999, vol. I (Dijon), Math. Phys. Stud. 21, Kluwer, Dordrecht, 2000, 255–307.

[7] R. C. Lindenbergh, *Limits of Voronoi diagrams*, Ph.D. thesis, Utrecht University, arXiv: `xxx-MG/0210345`, 2002.

[8] A. Okabe, B. Boots, K. Sugihara, S. N. Chiu, *Spatial Tessellations: Concepts and Applications of Voronoi Diagrams*, second ed., Wiley, Chichester, 2000.

[9] D. Siersma, *Isolated line singularities*, in: Singularities, Part 2, Proc. Sympos. Pure Math. 40, Amer. Math. Soc., Providence, 1983, 485–496.